CAMBRIDGE
UNIVERSITY PRESS

PAPER

Fractional order for the transmission dynamics of coffee berry diseases (CBD)

Abayneh Kebede Fantaye [ORCID]

Department of Mathematics, Debre Tabor University, Debre Tabor, Ethiopia
Email: abayk400@gmail.com

Abstract

Coffee berry diseases (CBD) pose significant threats to coffee production worldwide, affecting the livelihoods of millions of farmers and the global coffee market. Fractional calculus provides a powerful framework for describing non-local and memory-dependent phenomena, making it suitable for modelling the long-range interactions inherent in CBD spread. This study aims to formulate and analyse fractional order model for CBD transmission dynamics in the sense of Atangana–Baleanu–Caputo. Fixed point theorems were utilised to test the existence and uniqueness of the model's solutions using fractional order. The basic reproduction number was calculated utilising the next-generation matrix. The model has locally asymptotically stable equilibrium positions (disease-free and endemic). Furthermore, the Lyapunov function was used to conduct a global stability analysis of the equilibrium locations. A numerical simulation of the CBD model was created using the fractional Adam–Bashforth–Moulton approach to validate the analytical findings. Our findings contribute to the development of more accurate predictive models and inform the design of targeted interventions to mitigate the impact of CBD on coffee production systems.

1. Introduction

Coffee is a cultivar that grows well in the varied eco-physiological conditions of tropical and subtropical highlands and can be grown on agricultural land. After crude oil, it is the most consumed beverage and the second most traded commodity worldwide [45]. Although it is the main source of income for tropical countries, which are often less developed, wealthy countries are the ones that consume it the most [23]. The growth of weeds, pests and diseases have all hampered coffee output. For example, the coffee berry disease (CBD) caused by Colletotrichum kahawae substantially hinders the production of Arabica coffee in African countries [51]. It is a pathogenic fungus that affects plants [9, 32]. Black depressed wounds on coffee berries are one of the signs of CBD [22]. All phases of fruit and flower development are affected by the disease, but immature berries are especially vulnerable during the 4–16 weeks expanding phase following flowering [41].

The quality and yield of coffee berries are both affected by this disease. In this regard, Ethiopia, Kenya and Cameroon each decrease in up to 29, 9, 75 and 60% of their annual output, respectively. In regions with high levels of precipitation, humidity and altitude, losses could reach 100% [23, 3]. Biological control, pharmacological treatments, cultural customs, the adoption of resistant cultivars and other approaches are some of the various ways that CBD can be managed [24]. By way of the wind and rain, CBD is dispersed locally between branches and coffee trees [26] (see Figure 1). However, insects, birds and coffee harvesters are frequently used vectors for long- and medium-distance CBD dispersal

Figure 1. *Infected coffee berries with coffee berry disease (CBD).*

[19]. Healthy coffee berries, after coming into touch with a fungal disease from the environment or coffee berries that have already been infected with CBD, were responsible for the spread of the disease.

The dynamics of plant disease have been studied by different authors ([40–52]). For instance, Fotsa et al. [15] introduction of mathematical modelling and best management of the anthracnose disease is a good example. Plant pathogen epidemiological models were examined by Cunniffe and Gilligan [21]. Foltso et al. [2] presented and analysed a mathematical model of the coffee berry borer with optimal control strategies. The results were demonstrated using a class of models that had been subjected to plant disease experimentation. Following that, an impulse control approach that corresponds to cultivation methods was included in this study, making it more broadly applicable [30]. An important factor in the control of pests is farmer awareness, as demonstrated by [2].

Coffee wilt disease, coffee leaf rust and CBD are the three most dangerous coffee diseases that Ethiopia faces as a threat to its coffee production. The development and analysis of a nonlinear deterministic mathematical model for CBD transmission dynamics in a coffee farm was done by [31]. It was looked into how fungus pathogens interacted with disease vectors and coffee plants. Additionally, authors [33] developed a mathematical model of CBD dynamics. They determined the fundamental reproduction number (R_0), computed the equilibrium points of the system model and showed that the CBD ends when $R_0 < 1$. Moreover, they have shown that if $R_0 > 1$, CBD remains in the population of coffee plants. The numerical simulation's results agree with the stability analysis's theoretical conclusions.

Fractional calculus has been investigated by numerous authors as having the potential to take the memory effect into account [38–6]. Based on data from the past and the present, this memory makes predictions. Compared to integer derivatives, this sets it apart. In order to handle issues in fractional calculus, which has numerous real-world applications, significant analytical and numerical approaches have been developed [42–37] and [8]. For investigating the impact of the memory effect on epidemiological models and generating more accurate results, fractional calculus is essential. Because fractional calculus was used so frequently, it was impossible to accurately depict a variety of inherited materials

and memory processes in the framework of mathematical modelling [12]. Due to their special characteristics, fractional differential equations (FDE) provide a number of advantages over integer-order differential equations (IDEs) when it comes to simulating difficult real-world problems. Unlike IDEs, which are based locally, FDEs are composed of memory effects, which contribute to their increased efficiency.

In a sense, it is more flexible than classical calculus because of its hereditary characteristics and the way memory is described [27]. The Caputo fractional derivative (CFD), Caputo–Fabrizio derivative, Atangana–Baleanu fractional derivative and many others are introduced in this tool for use in modelling. The various kernels available for fractional derivatives, which can be selected to meet the needs of various applications, are the fundamental differences between them. The key distinction between the CFD [17], Caputo–Fabrizio derivative [13] and Atangana–Baleanu fractional derivative [4] is that the Caputo derivative is defined by a power law, the Caputo–Fabrizio derivative by an exponential decay law and the Atangana–Baleanu derivative by a Mittag-Leffler law. In fractional derivatives, several studies have recently been developed. One of the best operators is the Atangana–Baleanu–Caputo (ABC) operator [10]. An expanded Mittag-Leffler function with a non-singular and non-local kernel serves as the foundation for this operator.

Nevertheless, no previous research has used a fractional order to predict the kinetics of CBD transmission. In this study, we will incorporate the non-singular kernel of the Atangana–Baleanu fractional derivative to build a new model for the analysis of CBD [7]. This unique fractional operator is considered since it does not suffer from the singularity that arises from using other fractional derivatives. When simulating biological and physical processes, the Atangana–Baleanu fractional derivative is the most popular method since it does not involve the singularity associated with non-singular and non-local kernels [7]. Furthermore, equilibria based on the value of the fundamental reproduction number (R_0) are studied with respect to their local and global asymptotic stability. The remaining sections of the paper are organised as follows: Some initial ideas and the model's formulation are covered in parts two and three, respectively. In parts four and five, respectively, the equilibrium points and stability analysis of CBD are established. Additionally, in parts six and seven, respectively, the numerical solution and numerical simulation of the model are examined. Part eight concludes with some final thoughts.

2. Preliminaries

Now let's begin by reviewing the fundamental definitions of Atangana–Baleanu fractional operators.

Definition 1. *Let $f \in C^1(\alpha, \beta), \alpha < \beta$, be a function, and let $\sigma \in [0, 1]$. The ABC fractional derivative of order σ is given by [43–45]*

$$_{\alpha}^{ABC}D_t^{\sigma}f(t) = \frac{G(\sigma)}{1 - \sigma} \int_{\alpha}^{t} \frac{df}{dn} E_{\sigma}\left[-\frac{\sigma}{1 - \sigma}(t - n)^{\sigma}\right] dn, \tag{1}$$

where $G(\sigma)$ is the normalisation function given by $G(\sigma) = 1 - \sigma + \frac{\sigma}{\Gamma(\sigma)}$, characterised by $G(0) = G(1) = 1$, and the Mittag-Leffler function $E_{\sigma}(z)$ with $\mathbb{C}$ the set of the complex number is given by

$$E_{\sigma}(z) = \sum_{b=0}^{\infty} \frac{z^b}{\Gamma(1 + \sigma b)}, \sigma, b \in \mathbb{C}, \mathbb{R}(\sigma) > 0. \tag{2}$$

Definition 2. *The ABC fractional integral of the function $f \in C^1(\alpha, \beta)$ is given by [44, 45]*

$$_{\alpha}^{AB}I_t^{\sigma}f(t) = \frac{1 - \sigma}{G(\sigma)}f(t) + \frac{\sigma}{G(\sigma)\Gamma(\sigma)} \int_{\alpha}^{t} f(n)(t - n)^{\sigma - 1}dn. \tag{3}$$

Lemma 1. [46]: *The ABC fractional derivative and ABC fractional integral of the function $f \in C^1(\alpha, \beta)$ satisfies the Newton–Leibniz equality*

$$_{\alpha}^{AB}I_t^{\sigma}\left(_{\alpha}^{ABC}D_t^{\sigma}f(t)\right) = f(t) - f(\alpha).$$

Lemma 2. [47]: *Assume that for $0 < \sigma \leq 1, f(t) \in C(\alpha, \beta)$. If ${}_{t_0}^{ABC}D_t^\sigma f(t) \geq 0 \left({}_{t_0}^{ABC}D_t^\sigma f(t) \leq 0 \right), t \in (a, b),$ then $f(t)$ is a increasing (decreasing) function for $t \in [a, b]$.*

Lemma 3. [48]: *For two functions $f, g \in \mathbb{K}^1(\alpha, \beta), \alpha < \beta$, the AB fractional derivative satisfies the following inequality:*

$$\|{}_{\alpha}^{ABC}D_t^\sigma f(t) - {}_{\alpha}^{ABC}D_t^\sigma g(t)\| \leq \mathbb{K}\|f(t) - g(t)\|.$$

Lemma 4. (Generalised mean value theorem, [49]): *Let $f(x) \in C[\alpha, \beta]$, and let ${}_0^{ABC}D_t^\sigma f(x) \in C[\alpha, \beta]$ when $0 < \sigma \leq 1$. Then we have $f(x) = f(\alpha) + \frac{1}{\Gamma(\sigma)} {}_0^{ABC}D_t^\sigma f(\phi)(x - \phi)^n$, when $0 \leq \phi \leq x, \forall x \in (\alpha, \beta]$. Note that by Lemma 3, if $f(x) \in [0, \beta], {}_0^{ABC}D_t^\sigma f(x) \in C[0, \beta]$ and ${}_0^{ABC}D_t^\sigma f(x) \geq 0, \forall x \in (0, \beta]$ when $0 \leq \sigma \leq 1$, then the function $f(x)$ is non-decreasing, and if ${}_0^{ABC}D_t^\sigma f(x) \leq 0, \forall x \in (0, \beta]$, then the function $g(x)$ is non-increasing $\forall x \in (0, \beta]$.*

Then, next, we will proceed to the formulation of the model.

3. Formulation of the model

In this work, we partitioned the CBD model into coffee berry and vector populations. There are susceptible and infected coffee berry subcategories in the total coffee berry population ($N_c(t)$). Susceptible coffee berry is denoted by S_c, and infected coffee berry is denoted by I_c. This is defined as $N_c(t) = S_c + I_c$. There are susceptible and infected subclasses in the total vector population ($N_v(t)$). The susceptible vector is represented by S_v, and the infected vector is represented by I_v. This is defined as $N_v(t) = S_v + I_v$. The model took into account the recruitment rate of susceptible vectors r_2 and the shift to infected vectors (I_v) with β_2 rate after eating ill plants or coffee berry. The susceptible coffee berry (S_c) is also replanted at a rate of rr_1, and the diseases spread to coffee berry, and when infected vectors (Y_v) eat susceptible cotton (S_c), the diseases propagate to coffee berry at a rate of β_1. Coffee berry, once infected, never recovers and produces no or extremely low yields. To regulate the illness, the parameter γ is the induced death rate and is the elimination rate of infected coffee berry from uninfected coffee berry. Furthermore, d and μ are the natural death rates of coffee berry and vector population, respectively.

The following governing equations are given based on the model's assumptions and flow chart in Figure 2:

$$\frac{dS_c}{dt} = r_1 - \beta_1 S_c I_v - dS_c,$$

$$\frac{dI_c}{dt} = \beta_1 S_c I_v - (d + \gamma)I_c,$$

$$\frac{dS_v}{dt} = r_2 - \beta_2 I_c S_v - \mu S_v,$$

$$\frac{dI_v}{dt} = \beta_2 I_c S_v - \mu I_v. \tag{4}$$

Now, replacing the $\frac{d}{dt}$ in the system (4) with ${}_0^{ABC}D_t^\sigma$, we obtain the AB derivative that is described by the system of differential equations given in equation (5).

$$
\begin{aligned}
{}_0^{ABC}D_t^\sigma S_c(t) &= r_1 - \beta_1 S_c I_v - dS_c,\\
{}_0^{ABC}D_t^\sigma I_c(t) &= \beta_1 S_c I_v - (d + \gamma)I_c,\\
{}_0^{ABC}D_t^\sigma S_v(t) &= r_2 - \beta_2 I_c S_v - \mu S_v,\\
{}_0^{ABC}D_t^\sigma I_v(t) &= \beta_2 I_c S_v - \mu I_v,
\end{aligned}
\tag{5}
$$

with initial conditions

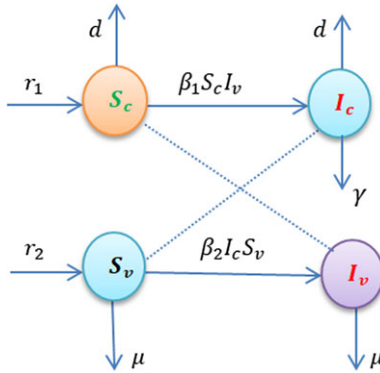$$S_c(0) > 0, I_c(0) \geq 0, S_v(0) \geq 0, I_v(0) \geq 0. \tag{6}$$

Figure 2. *Flow chart of the model.*

3.1. Existence and uniqueness of solutions

In this subsection, we shall apply some basic results from fixed point theory to the model (1), in order to establish the existence and uniqueness of the solution. The model (1) is rewritten in the following form:

$$\begin{cases} {}^{ABC}_{\alpha}D^{\sigma}_t G(t) &= g(t, G(t)), \\ g(0) &= g_0. \end{cases} \tag{7}$$

where the vector $g = (S_c, I_c, S_v, I_v)$ represents the compartments of the model and g denotes a continuous vector defined as follows:

$$g = \begin{pmatrix} g_1 \\ g_2 \\ g_3 \\ g_4 \end{pmatrix} = \begin{pmatrix} r_1 - \beta_1 S_c I_v - dS_c \\ \beta_1 S_c I_v - (d + \gamma)I_c \\ r_2 - \beta_2 I_c S_v - \mu S_v \\ \beta_2 I_c S_v - \mu I_v \end{pmatrix}. \tag{8}$$

The initial condition of the variables of the model is denoted by $g(0) = (S_c(0), I_c(0), S_v(0), I_v(0))$. Furthermore, G satisfies the Lipschitz condition as given by Lemma 3:

$$\|g(t, g_1(t)) - g(t, g_2(t))\| \le K \|g_1(t) - g_2(t)\|. \tag{9}$$

The existence of the solution for model equation (5) is investigated in the following theorem:

Theorem 1. *There exists a unique solution in $C^1([0, T])$ to the initial value problem $t \in [0, T]$ given that equation (9) and*

$$\left(\frac{(1-\sigma)K}{G(\sigma)} + \frac{\sigma K}{G(\sigma)\Gamma(\sigma + 1)} T^{\sigma}_{\max} \right) < 1. \tag{10}$$

are satisfied.

Proof. Applying ABC fractional integral on both sides of equation (18), we obtain

$$g(t) = g_0 + \frac{1-\sigma}{G(\sigma)} g(t, g(t)) + \frac{\sigma}{G(\sigma)\Gamma(\sigma)} \int_0^t (t - \tau)^{\sigma-1} g(t, g(t)) d\tau. \tag{11}$$

Let $M = (0, K)$. Then, define the operator $\mathcal{F} : C(M, \mathbb{R}^4) \to C(M, \mathbb{R}^4)$ by

$$\mathcal{F}[g(t)] = g_0 + \frac{1-\sigma}{G(\sigma)} g(t, g(t)) + \frac{\sigma}{G(\sigma)\Gamma(\sigma)} \int_0^t (t - \tau)^{\sigma-1} g(t, g(t)) d\tau. \tag{12}$$

It implies that $g(t) = \mathcal{F}[g(t)]$. The supremum norm on $M.\|.\|_M$ is given by

$$\|g(t)\|_M =_{t \in M}^{\sup} \|g(t)\|, g(t) \in C. \tag{13}$$

Clearly, $C(M, \mathbb{R}^4)$ equipped with $\|.\|_M$ is a Banach space. Also, the following inequality holds

$$\| \int_0^t B(t, \tau)g(\tau)d\tau \| \leq \|B(t, \tau)\|_M \|g(t)\|_M, \tag{14}$$

with $g(t) \in C(M, \mathbb{R}^4)$, $B(t, \tau) \in C(M^2, \mathbb{R})$ such that $|B(t, \tau)|_M =_{t, \tau \in M}^{\sup} |B(t, \tau)|$. By applying equation (9), we have that

$$\|\mathcal{F}(g_1(t)) - \mathcal{F}(g_2(t))\|_M \leq \| \frac{1 - \sigma}{G(\sigma)} (g(t, g_1(t)) - g(t, g_2(t)))$$

$$+ \frac{\sigma}{G(\sigma)\Gamma(\sigma)} \int_0^t (t - \tau)^{\sigma - 1} (g(\tau, g_1(\tau)) - g(\tau, g_2(\tau))) \, d\tau \|,$$

$$\leq \frac{1 - \sigma}{G(\sigma)} K \|g_1(t) - g_2(t)\| + \frac{\sigma K}{G(\sigma)\Gamma(\sigma)} \int_0^t (t - \tau)^{\sigma - 1} \|g_1(t) - g_2(t)\| d\tau,$$

$$\leq \frac{1 - \sigma}{G(\sigma)} K \sup |_{g \in [0,T]} \|g_1(t) - g_2(t)\| \tag{15}$$

$$+ \frac{\sigma K}{G(\sigma)\Gamma(\sigma)} \left(\int_0^t (t - \tau)^{\sigma - 1} \right) d\tau \sup |_{g \in [0,T]} \|g_1(\tau) - g_2(\tau)\|,$$

$$\leq \left(\frac{(1 - \sigma)K}{G(\sigma)} + \frac{\sigma K T_{\max}^\sigma}{G(\sigma)\Gamma(\sigma + 1)} \right) \|g_1(t) - g_2(t)\|. \tag{16}$$

Consequently, if the condition in equation (10) is satisfied, then $\|\mathcal{F}([g_1(t)]) - \mathcal{F}([g_2(t)])\| < \|g_1(t) - g_2(t)\|$ and the operator $\mathcal{F}$ become a contraction. Hence, $\mathcal{F}$ has a unique fixed point, which is a solution to the initial value problem in (18) and thus a solution to the system of equation (5). □

Theorem 2. *For the initial condition given in (6), the solution of the system of equation (5) is non-negative and bounded for $t > 0$ in the region*

$$\Omega = \Omega_c \times \Omega_v = \left\{ (S_c, I_c, S_v, I_v) \in \mathbb{R}_+^4 : N_c \leq \frac{r_1}{d}, N_v \leq \frac{r_1}{\mu} \right\}. \tag{17}$$

Proof. First, we shall prove that $S_c(t) > 0$ for all $t \geq 0$. We assume that $S_c(t) \geq 0$ is not true. Then there exists at $\tau_1 > 0$, such that

$$\begin{cases} S_c(t) > 0 & \text{for } t_0 \leq t < \tau_1, \\ S_c(t) = 0 & \text{for } t = \tau_1, \\ S_c(t) < 0 & \text{for } \tau_1 < t < \tau_1 + \varepsilon \text{ for } \varepsilon > 0. \end{cases} \tag{18}$$

Then, from the first system of equation (5), we have

$${}_0^{ABC}D_t^\sigma S_c|_{S_c=0} = r_1 \geq 0. \tag{19}$$

Thus, using Lemma 2, for all $0 < \varepsilon << 1$, we have $S_c(\tau_1 + \varepsilon) = S_c(\tau_1) + \frac{1}{\sigma}\frac{d^\sigma}{dt^\sigma}S_c(t)\varepsilon^\sigma$. Hence, $S_c(\tau_1 + \varepsilon) > 0$ contradicts our assumption that $S_c(t) < 0$ for $\tau_1 < t < \tau_1 + \varepsilon$ for $\varepsilon > 0$. As a result, we obtain $S_c(t) \geq 0$ for all $t \geq 0$. Similarly, we have $I_c(t) \geq 0, S_v(t) \geq 0, I_v(t) \geq 0$, for all $t \geq 0$. It follows that each of the solutions of (5) is non-negative and remains in $\mathbb{R}_+^4$, and hence, the set Ω defined in (17) is positively invariant for model (5). □

Eventually, to demonstrate the boundedness of the fractional model's solutions (5), given that all of the parameters are positive, we continue by adding up all of the model's equations for both cotton and

vector population, which yields

$$\,_{0}^{ABC}D_t^\sigma N_c = r_1 - dN_c - \gamma I_c \le r_1 - dN_c, \tag{20}$$

$$\,_{0}^{ABC}D_t^\sigma N_v = r_2 - \mu N_v. \tag{21}$$

Now, using the Laplace transform and simplifying equations (20) and (21), we get

$$N_c(t) \le \left(\frac{G(\sigma)}{G(\sigma) + (1-\sigma)d} N_c(0) + \frac{(1-\sigma)r_1}{G(\sigma) + (1-\sigma)d} \right) E_{\sigma,1} \left(-c_1 t^\sigma \right)$$
$$+ \frac{\sigma r_1}{G(\sigma) + (1-\sigma)d} E_{\sigma,\sigma+1} \left(-c_2 t^\sigma \right), \tag{22}$$

$$N_v(t) \le \left(\frac{G(\sigma)}{G(\sigma) + (1-\sigma)\mu} N_v(0) + \frac{(1-\sigma)r_2}{G(\sigma) + (1-\sigma)\mu} \right) E_{\sigma,1} \left(-c_2 t^\sigma \right)$$
$$+ \frac{\sigma r_2}{G(\sigma) + (1-\sigma)\psi} E_{\sigma,\sigma+1} \left(-c_2 t^\sigma \right), \tag{23}$$

where $c_1 = \frac{\sigma d}{G(\sigma) + (1-\sigma)d}$ and $c_2 = \frac{\sigma \mu}{G(\sigma) + (1-\sigma)\mu}$ with E_{σ,c_1} and E_{σ,c_2} constitute the two parameter Mittag-Leffler function and due to its asymptotic nature that leads to the conclusion that $N_c(t) \le \frac{r_1}{d}$ and $N_v(t) \le \frac{r_2}{\mu} ast \to \infty$. Hence, (17) is the biologically feasible region of model (5).

4. Equilibrium points of the model

4.1. The coffee berry disease-free equilibrium points of the model (E_0)

The CBD-free equilibrium points (E_0) of the model are stationary solutions with no diseases. It is obtained by equating equation (5) to zero and using $I_c = 0$ and $Y_v = 0$. Then, E_0 of our model equation (5) is given by

$$E_0 = (S_c^0, I_c^0, S_v^0, I_v^0) = \left(\frac{r_1}{d}, 0, \frac{r_2}{\mu}, 0 \right). \tag{24}$$

4.2. The basic reproduction number (R_0)

The basic reproduction number (R_0) counts the estimated number of secondary infections that result from one newly infected coffee berry delivered directly into a susceptible population. We can obtain R_0 of the system of equation (5) using the next-generation matrix method as described by [50]. It can be determined by rewriting the system of equation (5) starting with newly infective classes and using the next-generation matrix method:

$$\,_{0}^{ABC}D_t^\sigma I_c = \beta_1 S_c I_v - (d + \gamma) I_c, \tag{25}$$

$$\,_{0}^{ABC}D_t^\sigma I_v = \beta_2 I_c S_v - \mu I_v. \tag{26}$$

Then, we consider

$$\boldsymbol{f} = \begin{pmatrix} \beta_1 S_c I_v \\ \beta_2 I_c S_v \end{pmatrix}, \boldsymbol{v} = \begin{pmatrix} (d+\gamma)I_c \\ \mu I_v \end{pmatrix} \tag{27}$$

Now, the Jacobian matrix of $\boldsymbol{f}$ and $\boldsymbol{v}$ with respect to I_c and I_v at CBD-free equilibrium point $E_0 = \left(\frac{r_1}{d}, 0, \frac{r_2}{\mu}, 0 \right)$ is

$$\mathbb{F} = \begin{pmatrix} 0 & \frac{\beta_1 r_1}{d} \\ \frac{\beta_2 r_2}{\mu} & 0 \end{pmatrix}, \mathbb{V} = \begin{pmatrix} d+\gamma & 0 \\ 0 & \mu \end{pmatrix}. \tag{28}$$

Then, by the principle of next-generation matrix, basic reproduction number (R_0) is the dominant eigenvalue of the FV^{-1} or spectral radius of FV^{-1} where

$$FV^{-1} = \begin{pmatrix} 0 & \frac{\beta_1 r_1}{d} \\ \frac{\beta_2 r_2}{\mu} & 0 \end{pmatrix} \begin{pmatrix} \frac{1}{d+\gamma} & 0 \\ 0 & \frac{1}{\mu} \end{pmatrix} = \begin{pmatrix} 0 & \frac{\beta_1 r_1}{d\mu} \\ \frac{\beta_2 r_2}{\mu(d+\gamma)} & 0 \end{pmatrix}. \tag{29}$$

The characteristic equations of equation (29) becomes

$$\lambda^2 - \frac{m_1 r_2 \beta_1 \beta_2}{(d+\gamma)d\mu^2} = 0 \implies \lambda = \pm\sqrt{\frac{r_1 r_2 \beta_1 \beta_2}{(d+\gamma)d\mu^2}}. \tag{30}$$

Since, R_0 is the maximum eigenvalues of FV^{-1} or the spectral radius of FV^{-1}. That is,

$$R_0 = \max\left\{-\sqrt{\frac{r_1 r_2 \beta_1 \beta_2}{(d+\gamma)d\mu^2}}, \sqrt{\frac{r_1 r_2 \beta_1 \beta_2}{(d+\gamma)d\mu^2}}\right\}. \tag{31}$$

4.3. Coffee berry disease endemic equilibrium point of the model (E_1)

The coffee berry endemic equilibrium point, $E_1 = (S_c^*, I_c^*, S_v^*, I_v^*)$, of the model is the steady-state solution, where coffee berries persist in the population of coffee plants. We can obtain this by equating each system of equation (5) equal to zero, and it is given by

$$S_c^* = \frac{r_1(r_1\beta_2 + \mu(d+\gamma))}{d\mu(d+\gamma)(R_0^2 - 1) + d(r_1\beta_2 + \mu(d+\gamma))}, \tag{32}$$

$$I_c^* = \frac{r_1\mu(R_0^2 - 1)}{\mu((d+\gamma))(R_0^2 - 1) + (r_1\beta_2 + \mu(d+\gamma))}, \tag{33}$$

$$S_v^* = \frac{r_2((d+\gamma)\mu(R_0^2 - 1) + r_1\beta_2 + d\mu)}{\mu((r_1\beta_2 + d\mu)(R_0^2 - 1) + r_1\beta_2 + \mu(d+\gamma))}, \tag{34}$$

$$I_v^* = \frac{d\mu(d+\gamma)(R_0^2 - 1)}{\beta_1(r_1\beta_2 + \mu)(d+\gamma)}. \tag{35}$$

5. Stability analysis of the model

5.1. Local stability of the coffee berry disease-free equilibrium point

The linearisation system of equation (5) at E_0 can be used to find the local stability of the model at E_0.

Theorem 3. *Disease-free equilibrium point (E_0) of the system of equation (5) is locally asymptotically stable, if $R_0 < 1$.*

Proof. Evaluating the Jacobian matrix of the system of equation (5) at $E_0 = \left(\frac{r_1}{d}, 0, \frac{r_2}{\mu}, 0\right)$ is

$$J(E_0) = \begin{pmatrix} -d & 0 & 0 & -\frac{\beta_1 r_1}{d} \\ 0 & -(d+\gamma) & 0 & \frac{\beta_1 r_1}{d} \\ 0 & -\frac{\beta_2 r_2}{\mu} & -\mu & 0 \\ 0 & \frac{\beta_2 r_2}{\mu} & 0 & -\mu \end{pmatrix}. \tag{36}$$

The corresponding characteristic equation of the Jacobian matrix of equation (36) at E_0 is given by $|J(E_0) - \lambda I_4| = 0$. That is,

$$(-d - \lambda)(-\mu - \lambda)(\lambda^2 + d_1\lambda + d_2) = 0. \tag{37}$$

where

$$d_1 = d + \gamma + \mu,$$

$$d_2 = (d+\gamma)\mu - \frac{r_1 r_2 \beta_1 \beta_2}{d\mu} = (d+\gamma)\mu \left[1 - \frac{r_1 r_2 \beta_1 \beta_2}{(d+\gamma)d\mu^2}\right] = (d+\gamma)\mu(1 - R_0^2). \tag{38}$$

Clearly, from equation (37), we observe that

$$\lambda_1 = -d < 0, \lambda_2 = -\mu < 0, \tag{39}$$

and from the last expression of equation (37), that is,

$$\lambda^2 + d_1\lambda + d_2 = 0, \tag{40}$$

by using the Routh–Hurwitz criteria, equation (40) has a strictly negative real root if $d_1 > 0$ and $d_2 > 0$. Clearly, we observe that $d_1 = d + \gamma + \mu > 0$ and

$$d_2 = (d+\gamma)\mu(1 - R_0^2) > 0, \tag{41}$$

if $(1 - R_0^2) > 0$. That is, $R_0^2 < 1$ implies that $R_0 < 1$. As a result, our model equation (5) at E_0 offers all eigenvalues with a negative real part, and so it is locally asymptotically stable if $R_0 < 1$. □

5.2. Global stability of the coffee berry disease-free equilibrium point

To establish the global stability of disease-free equilibrium point (E_0), we need to rewrite the system of equation (5) in the following form:

$$\dot{M} = J(M, L),$$
$$\dot{L} = P(M, L),$$
$$P(M, 0) = 0, \tag{42}$$

where $M = (S_c, S_v) \in R^2$ represents the number of uninfected classes, while $L = (I_c, I_v) \in R^2$ represents the number of infected classes, and $E_0 = (M^0, 0)$ represents the CBD-free equilibrium of this system. The disease-free equilibrium E_0 is a globally asymptotically stable equilibrium for the model if the following conditions are fulfilled:

1. $\frac{dM}{dt} = J(M, 0), M^*$ is a globally asymptotically stable.
2. $\frac{dL}{dt} = D_L P(M^*, 0)L - P_1(M, L), P_1(M, L) \geq 0, \forall (M, L) \in \Omega.$

where $D_L P(M^0, 0)$ is an M-matrix and $P(M, L)$ taken in (I_c, Y_v) and evaluated at $(M^0, 0) = \left(\frac{r_1}{d}, \frac{r_2}{\mu}, 0, 0\right)$. If the system of equation (42) satisfies the above conditions, then the following theorem holds.

Theorem 4. *The coffee berry disease-free equilibrium point, $E_0 = (M^0, 0)$, of the system of equation (5) is globally asymptotically stable if $R_0 \leq 1$ and conditions (1) and (2) are satisfied.*

Proof. From our model of equation (5), we can obtain $J(M, L)$ and $P(M, L)$:

$$J(M, L) = \begin{pmatrix} r_1 - \beta_1 S_c I_v - dS_c \\ r_2 - \beta_2 I_c S_v - \mu S_v \end{pmatrix},$$

$$P(M, L) = \begin{pmatrix} \beta_1 S_c I_v - (d + \gamma)I_c \\ \beta_2 I_c S_v - \mu I_v \end{pmatrix}.$$

Now, we consider the reduced system and from condition (1):

$$_0^{ABC}D_t^\sigma S_c = r_1 - dS_c, \tag{43}$$

$$\begin{aligned}{}_{0}^{ABC}D_{t}^{\sigma}S_{v} = r_2 - \mu S_v,\end{aligned} \tag{44}$$

$M^0 = \left(\frac{r_1}{d}, \frac{r_2}{\mu}\right)$ is a globally asymptotically stable equilibrium point for the reduced system $\frac{dM}{dt} = J(M, 0)$. Using the Laplace transform, the solution of equation (43) is $S_c(t) = \frac{r_1}{d} + \left(S_c(0) - \frac{r_1}{d}\right)e^{-dt}$, which approaches $\frac{r_1}{d}$ as $t \to \infty$, and from equation (44), we obtain $S_v(t) = \frac{r_2}{\psi} + (S_v(0) - \frac{r_2}{\mu})e^{-\mu t}$, which approaches $\frac{r_2}{\mu}$ as $t \to \infty$. Note that this asymptomatic dynamics is independent of the initial conditions in Ω; therefore, the convergence of the solutions of the reduced system (43) and (44) is global in Ω. Now, we compute

$$D_L P(M^0, 0) = \begin{pmatrix} -(d+\gamma) & \frac{r_1\beta_1}{d} \\ \frac{r_2\beta_2}{\mu} & -\mu \end{pmatrix}. \tag{45}$$

Then, $P(M, L)$ can be written as

$$P(M, L) = D_L P(M^*, 0)L - P_1(M, L), \tag{46}$$

and we want to show $P_1(M, L)$, which is obtained as

$$P_1(M, L) = \begin{pmatrix} \beta_1 I_v \left(\frac{r_1}{d} - S_c\right) \\ \beta_2 I_c \left(\frac{r_2}{\mu} - S_v\right) \end{pmatrix}. \tag{47}$$

Here $\frac{r_1}{d} \geq S_c$ and $\frac{r_2}{\mu} \geq S_v$. Hence, it is clear that $P_1(M, L) \geq 0, \forall (M, L) \in \Omega$. Thus, this proves that E_0 is globally asymptotically stable when $R_0 \leq 1$. $\qquad\square$

5.3. Local stability of the coffee berry endemic equilibrium point

We used the Jacobian stability approach to prove the local stability of the disease endemic equilibrium state in this section.

Theorem 5. *When $R_0 > 1$, the model's endemic equilibrium point, E_1, is locally asymptotically stable.*

Proof. The local stability of the coffee berry endemic equilibrium (E_1) is determined based on the signs of the eigenvalues of the Jacobian matrix, which is computed at E_1. Now, the Jacobian matrix of our model at E_1 is given by

$$J = \begin{pmatrix} -(\beta_1 I_v^* + d) & 0 & 0 & -\beta_1 S_c^* \\ \beta_1 I_v^* & -(d+\gamma) & 0 & \beta_1 S_c^* \\ 0 & -\beta_2 S_v^* & -(\beta_2 I_c^* + \mu) & 0 \\ 0 & \beta_2 S_v^* & \beta_2 I_c^* & -\mu \end{pmatrix}. \tag{48}$$

The corresponding characteristic equation of the Jacobian matrix of equation (48) at E_1 is $|J(E_1) - \lambda I_4| = 0$. That is,

$$P(\lambda) = f_4\lambda^4 + f_3\lambda^3 + f_2\lambda^2 + f_1\lambda + f_0, \tag{49}$$

where

$$\begin{aligned}
& f_4 = 1, f_3 = 2d + 2\mu + \beta_1 I_v^* + \beta_2 I_c^*, \\
& f_2 = d\mu + (d+\mu)(d+\gamma+\mu)(d+\gamma)\mu + (2\mu+d)\beta_1 I_v^* + (2d+\mu)\beta_2 I_c^* + \beta_1\beta_2(I_c^* - S_c^* I_v^*), \\
& f_1 = \mu d(d+\gamma+\mu) + (d+\mu)(d+\gamma)\mu + (d\mu + (d+\mu)(d+\gamma))\beta_2 I_c^* + (d+\gamma+\mu)\mu\beta_1 I_v^* \\
& \qquad + (d+\mu)\beta_1\beta_2 I_c^* I_v^* - \beta_1\beta_2(d+\mu)S_c^* S_v^*, \\
& f_0 = \mu\beta_1\beta_2(d+\gamma)I_c^* S_v^* + \beta_1\mu^2(d+\gamma)I_v^* + \mu\beta_1\beta_2(d+\gamma)I_c^* + d\mu^2(d+\gamma) - d\mu\beta_1\beta_2 S_c^* S_v^*. \tag{50}
\end{aligned}$$

Using the Routh–Hurwitz criterion, all roots of a characteristic polynomial have negative real parts if and only if $f_4 > 0, f_3 > 0, f_2 > 0, f_1 > 0, f_0 >, f_3 f_2 > f_1$ and $f_1 f_2 f_3 > f_0 f_3^2 + f_1^2$ for $R_0 > 1$. Therefore, E_1 is locally asymptotically stable if $R_0 > 1$. □

6. Numerical solution of the model

In this section, we develop a numerical scheme for model (5) using the Toufik–Atangana rule detailed in [49]. Now from the first equation of (5), we have

$$
\begin{aligned}
{}^{ABC}_0 D^\sigma_t S_c &= F_1(t, S_c(t)), \\
S_c(0) &= S_{c0}.
\end{aligned}
\tag{51}
$$

Based on (11), we obtain the solution for (51) given in (52):

$$
S_c(t) = S_c(0) + \frac{1-\sigma}{G(\sigma)} F_1(t, S_c(t)) + \frac{\sigma}{G(\sigma)\Gamma(\sigma)} \int_0^t F_1(\rho, S_c(\rho))(t-\rho)^{\sigma-1} d\rho.
\tag{52}
$$

Applying Lagrange's interpolation polynomial on the interval $[t_k, t_{k+1}]$ to the equality $F_1(w, S_c(w)) = r_1 - \beta_1 S_c(w) Y_v(w) - d S_c(w)$ leads to

$$
\begin{aligned}
S_c k \approx \frac{1}{h} & \left[(w - t_{k-1}) F_1(t_k, S_c(t_k), I_c(t_k), S_v(t_k), I_v(t_k)) \right] \\
& - \frac{1}{h} \left[(w - t_k) F_1(t_{k-1}, S_c(t_{k-1}), I_c(t_{k-1}), S_v(t_{k-1}), I_v(t_{k-1})) \right],
\end{aligned}
\tag{53}
$$

where $h = t_k - t_{k-1}$. Now, substituting equation (53) into equation (52), we get

$$
\begin{aligned}
S_c(t_{s+1}) = {}& S_c(0) + \frac{1-\sigma}{G(\sigma)} F_1(t_k, S_c(t_k), I_c(t_k), S_v(t_k), I_v(t_k)) + \frac{\sigma}{G(\sigma)\Gamma(\sigma)} \\
& \sum_{j=1}^s \frac{F_1(t_j, S_c(t_j), I_c(t_j), S_v(t_j), I_v(t_j))}{h} \int_{t_j}^{t_{j+1}} (w - t_{j-1})(t_{s+1} - w)^{\sigma-1} dw + \frac{\sigma}{G(\sigma)\Gamma(\sigma)} \\
& \sum_{j=1}^s -\frac{F_1(t_{j-1}, S_c(t_{j-1}), I_c(t_{j-1}), S_v(t_{j-1}), I_v(t_{j-1}))}{h} \int_{t_j}^{t_{j+1}} (w - t_{j-1})(t_{s+1} - w)^{\sigma-1} dw, \\
= {}& S_c(0) + \frac{1-\sigma}{G(\sigma)} F_1(t_s, S_c(t_s), I_c(t_s), S_v(t_s), I_v(t_s)) + \frac{\sigma}{G(\sigma)\Gamma(\sigma)} \\
& \sum_{j=1}^s \frac{F_1(t_j, S_c(t_j), I_c(t_j), S_v(t_j), I_v(t_j))}{h} M_{j-1} + G(\sigma)\Gamma(\sigma) \\
& \sum_{j=1}^s -\frac{F_1(t_{j-1}, S_c(t_{j-1}), I_c(t_{j-1}), S_v(t_{j-1}), I_v(t_{j-1}))}{h} M_j,
\end{aligned}
\tag{54}
$$

where

$$
\begin{aligned}
M_{j-1} = \int_{t_j}^{t_{j+1}} (w - t_{j-1})(t_{s+1} - w)^{\sigma-1} dw = {}& -\frac{1}{\sigma} \left[(t_{j+1} - t_{j-1})(t_{s+1} - t_{j+1})^\sigma - (t_j - t_{j-1})(t_{s+1} - t_j)^\sigma \right] \\
& -\frac{1}{\sigma(\sigma+1)} \left[(t_{s+1} - t_{j+1})^{\sigma+1}(t_{s+1} - t_{j+1})^\sigma - (t_{s+1} - t_j)^{\sigma+1} \right],
\end{aligned}
\tag{55}
$$

$$M_j = \int_{t_j}^{t_{j+1}} (w - t_{j-1})(t_{s+1} - w)^{\sigma-1} dw = -\frac{1}{\sigma} \left[(t_{j+1} - t_{j-1})(t_{s+1} - t_{j+1})^{\sigma} \right]$$

$$- \frac{1}{\sigma(\sigma+1)} \left[(t_{s+1} - t_{j+1})^{\sigma+1} - (t_{s+1} - t_j)^{\sigma+1} \right]. \tag{56}$$

Moreover, substituting $t_j = jh$ into equations (55) and (56) gives

$$M_{j-1} = \frac{h^{\sigma+1}}{\sigma(\sigma+1)} \left[(s+1-j)^{\sigma}(s-j+2+\sigma) - (s-j)^{\sigma}(s-j+2+2\sigma) \right], \tag{57}$$

$$M_j = \frac{h^{\sigma+1}}{\sigma(\sigma+1)} \left[(s+1-j)^{\sigma+1} - (s-j)^{\sigma}(s-j+1+\sigma) \right]. \tag{58}$$

Finally, we can express equation (54) in terms of equations (57) and (58) as follows:

$$S_c(t_{s+1}) = S_c(t_0) + \frac{1-\sigma}{G(\sigma)} F_1(t_s, S_c(t_s), I_c(t_s), S_v(t_s), I_v(t_s)) + \frac{\sigma}{G(\sigma)\Gamma(\sigma)}$$

$$\times \sum_{j=1}^{s} \frac{F_1(t_j, S_c(t_j), I_c(t_j), S_v(t_j), I_v(t_j))}{\Gamma(\sigma+2)}$$

$$\times h^{\sigma} \left[(s+1-j)^{\sigma}(s-j+2+\sigma) - (s-j)^{\sigma}(s-j+2+2\sigma) \right] + \frac{\sigma}{G(\sigma)\Gamma(\sigma)}$$

$$\times \sum_{j=1}^{s} -\frac{F_1(t_{j-1}, S_c(t_{j-1}), I_c(t_{j-1}), S_v(t_{j-1}), I_v(t_{j-1}))}{\Gamma(\sigma+2)} \tag{59}$$

$$\times h^{\sigma} \left[(s+1-j)^{\sigma+1} - (s-j)^{\sigma}(s-j+1+\sigma) \right].$$

In the same way, we have the following equations for the remaining state variables:

$$I_c(t_{s+1}) = I_c(t_0) + \frac{1-\sigma}{G(\sigma)} F_2(t_s, S_c(t_s), I_c(t_s), S_v(t_s), I_v(t_s)) + \frac{\sigma}{G(\sigma)\Gamma(\sigma)}$$

$$\times \sum_{j=1}^{s} \frac{F_2(t_j, S_c(t_j), I_c(t_j), S_v(t_j), I_v(t_j))}{\Gamma(\sigma+2)}$$

$$\times h^{\sigma} \left[(s+1-j)^{\sigma}(s-j+2+\sigma) - (s-j)^{\sigma}(s-j+2+2\sigma) \right] + \frac{\sigma}{G(\sigma)\Gamma(\sigma)}$$

$$\times \sum_{j=1}^{s} -\frac{F_2(t_{j-1}, S_c(t_{j-1}), I_c(t_{j-1}), S_v(t_{j-1}), I_v(t_{j-1}))}{\Gamma(\sigma+2)} \tag{60}$$

$$\times h^{\sigma} \left[(s+1-j)^{\sigma+1} - (s-j)^{\sigma}(s-j+1+\sigma) \right].$$

Table 1. *The parameter values*

Parameter	Value day^{-1}	Source
r_1	9.00	Estimated
r_2	5.00	Estimated
β_1	0.0004	Estimated
β_2	0.0005	Estimated
d	0.04	[20]
γ	0.002	Estimated
μ	0.009	[31]

$$
\begin{aligned}
S_v(t_{s+1}) = {} & S_v(t_0) + \frac{1-\sigma}{G(\sigma)} F_3(t_s, S_c(t_s), I_c(t_s), S_v(t_s), I_v(t_s)) + \frac{\sigma}{G(\sigma)\Gamma(\sigma)} \\
& \times \sum_{j=1}^{s} \frac{F_3(t_j, S_c(t_j), I_c(t_j), S_v(t_j), I_v(t_j))}{\Gamma(\sigma+2)} \\
& \times h^{\sigma} \left[(s+1-j)^{\sigma}(s-j+2+\sigma) - (s-j)^{\sigma}(s-j+2+2\sigma) \right] + \frac{\sigma}{G(\sigma)\Gamma(\sigma)} \\
& \times \sum_{j=1}^{s} - \frac{F_3(t_{j-1}, S_c(t_{j-1}), I_c(t_{j-1}), S_v(t_{j-1}), I_v(t_{j-1}))}{\Gamma(\sigma+2)} \\
& \times h^{\sigma} \left[(s+1-j)^{\sigma+1} - (s-j)^{\sigma}(s-j+1+\sigma) \right].
\end{aligned} \tag{61}
$$

$$
\begin{aligned}
I_v(t_{s+1}) = {} & I_v(t_0) + \frac{1-\sigma}{G(\sigma)} F_4(t_s, S_c(t_s), I_c(t_s), S_v(t_s), I_v(t_s)) + \frac{\sigma}{G(\sigma)\Gamma(\sigma)} \\
& \times \sum_{j=1}^{s} \frac{F_4(t_j, S_c(t_j), I_c(t_j), S_v(t_j), I_v(t_j))}{\Gamma(\sigma+2)} \\
& \times h^{\sigma} \left[(s+1-j)^{\sigma}(s-j+2+\sigma) - (s-j)^{\sigma}(s-j+2+2\sigma) \right] + \frac{\sigma}{G(\sigma)\Gamma(\sigma)} \\
& \times \sum_{j=1}^{s} - \frac{F_4(t_{j-1}, S_c(t_{j-1}), I_c(t_{j-1}), S_v(t_{j-1}), I_v(t_{j-1}))}{\Gamma(\sigma+2)} \\
& \times h^{\sigma} \left[(s+1-j)^{\sigma+1} - (s-j)^{\sigma}(s-j+1+\sigma) \right].
\end{aligned} \tag{62}
$$

7. Numerical simulation

This section examines the effects of various fractional order values on the system of equation (5). In order to achieve this, we present a number of numerical simulations of the model that make use of a numerical method created by Toufic and Antagana, as shown in equations (59)–(62). The following initial conditions are used in the simulations and analysis: $S_c(0) = 700, I_c(0) = 150, S_v(0) = 100, I_v(0) = 180$. The values of the parameters are shown in Table 1.

Figure 3 depicts how populations of susceptible coffee berries rise asymptotically to the disease-free equilibrium point, while those of infected coffee berries fall asymptotically to that point. The susceptible vector population increases asymptotically to the disease-free equilibrium point, whereas the infected vector population decreases asymptotically to the same equilibrium point. In this case, the disease might ultimately go away in the long run. The fact that $R_0 = 0.0442$, which is less than one, accounts for the existence of such a condition. This indicates the theorem that the stability of the disease-free equilibrium
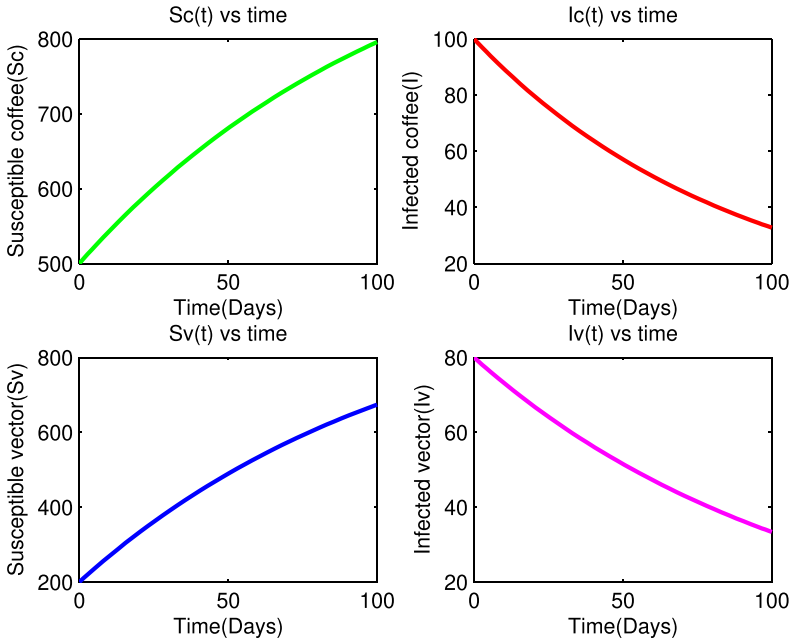
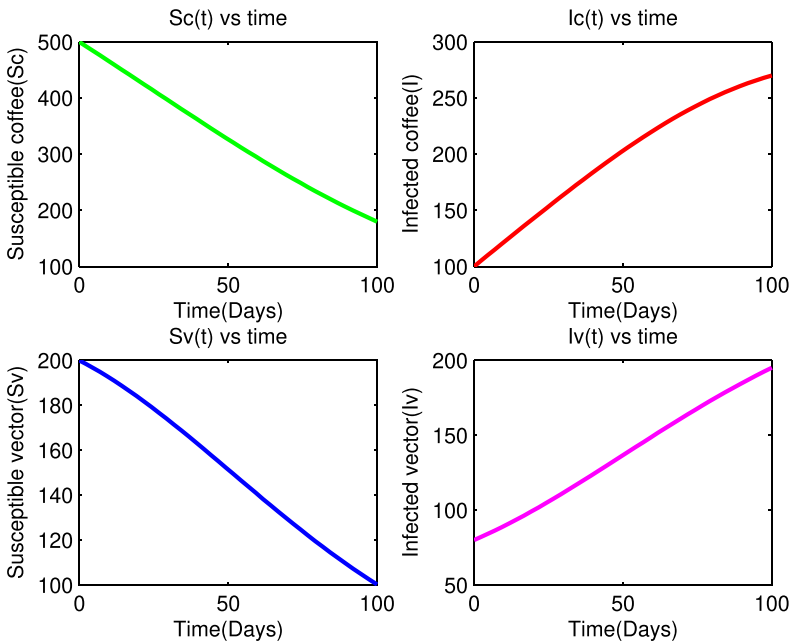**Figure 3.** *Time series plot of state variables for $R_0 < 1$.*

Figure 4. *Time series plot of state variables for $R_0 > 1$.*

point occurs when $R_0 < 1$; that is, if $R_0 < 1$, then on average, one infected coffee berry produces less than one newly infectious coffee berry over the course of its disease period. Figure 4 demonstrates how the number of susceptible coffee berry and vector decreases as a result of the influence of infected coffee berry and vector people, after which they join the infected class, leading to an increase in infected coffee berry and vector. As a result, the number of infected coffee berries and vectors is rising, and the disease's
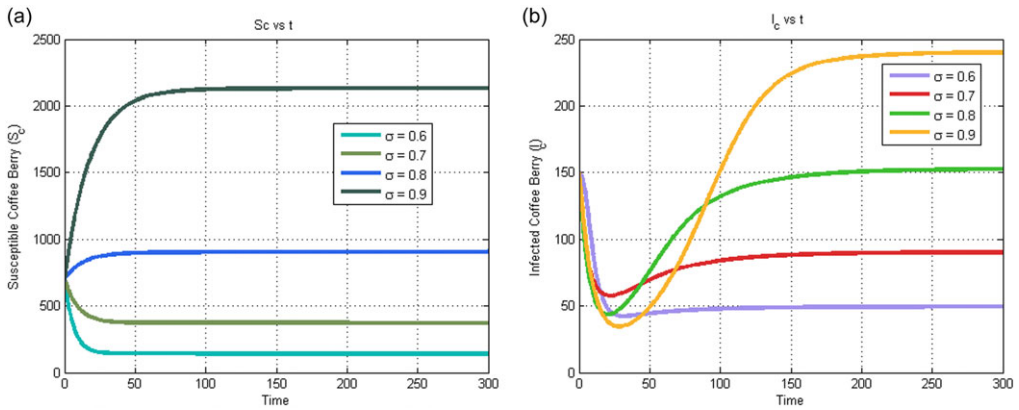
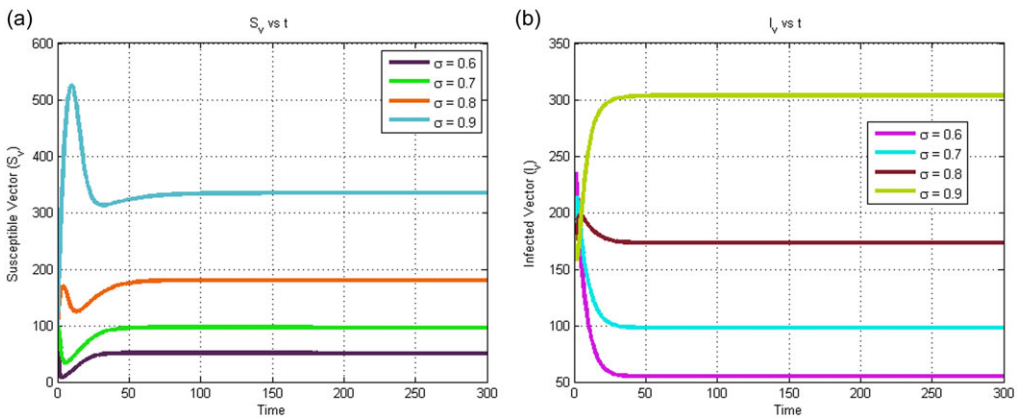**Figure 5.** *Total number of susceptible and infected coffee berry with different values of σ.*

Figure 6. *Total number of susceptible and infected vector with different values of σ.*

endemic equilibrium point is both present and stable. The fact that $R_0 = 5.3244$, which is greater than one, proves that this condition exists. This demonstrates the theorem that disease endemic equilibrium points are stable when $R_0 > 1$; that is, if each infected coffee berry and its vectors produce, on average, more than one new infected coffee berry and vector, then the disease can spread in the specified area. Figure 5a demonstrates how decreasing the number of coffee berries (S_c) that are susceptible results from increasing the fractional order (σ) from 0.04 to 1.00. Figure 5b demonstrates how increasing the fractional order (σ) from 0.04 to 1.00 results in an increase in the number of infected coffee berries (I_c). According to Figure 6a, the number of susceptible vector populations (S_v) decreases as fractional order (σ), increases from 0.04 to 1.00. The fractional order (σ) is shown in Figure 6b to increase from 0.04 to 1.00, which results in an increase in the population of infected vectors (I_v). To put it another way, we can infer from Figures 5 and 6 that a reduction in *sigma* results in a marked decrease in the number of I_c and I_v cases. The curves for each compartment, I_c and I_v, also compress as the value decreases from 1.00 to 0.04, as shown in the figures. Therefore, we can say that diseases in I_c and I_v decrease as one approaches zero from the right.

More specifically, the memory effect of the dynamic system is increased when the derivative order is decreased from 1.00 to 0.04, which causes the infection in each compartment to gradually worsen over time. As a result, we can infer from the results that lowering the derivative's fractional order significantly slows the growth of crop infections and that lowering it to zero produces no change in rate of change.

If the disease's rate of spread stays the same, the crop will produce. Because of this, the fractional order will be higher than 0. The role of farmer's experience or knowledge of the history of the disease is also captured by the derivative order. The approximative findings support the notion that fractional order derivatives offer a wealth of dynamics and frequently express biological systems more effectively. The results allow us to draw the conclusion that lowering the derivative's fractional order significantly slows the growth of crop infections and that lowering it to zero produces no change in rate of change. If there is no change in the disease's rate, the crop will produce. The fractional order will thus be higher than zero. Additionally, the derivative order captures the significance of farmer's expertise or familiarity with the disease's past. The rough results show that fractional order derivatives have a lot of dynamics and have an ability to better represent biological systems.

8. Conclusion

In this study, we looked into an Atangana–Baleanu fractional derivative-based mathematical model for eco-epidemiology. We established the existence and uniqueness of the solution, asymptotic stability of the equilibria and the fundamental reproduction number (R_0). The findings of the study, the CBD-free equilibrium is locally and globally asymptotically stable if the basic reproduction number is less than one; however, if the basic reproduction number is greater than one, the coffee berry endemic equilibrium is locally asymptotically stable. According to the simulation results, the graphs flattened as the fractional derivative order was decreased from 1.00, and the disease progresses slowly for the susceptible class (S_c). The graphs for compartments (I_c) and (I_v) demonstrate that the disease spreads gradually as the fractional order decreases, and the number of cases at maximum declines relatively. This noteworthy result is due to the fractional operator Atangana–Baleanu with the inherited assets. We claim that fractional models using the Atangana–Baleanu operator can shed more light on the hidden or actual characteristics of phenomena encountered in everyday life. As the order is decreased, we see a decrease in the number of cases as we display graphic results with various fractional orders. In the future study, the impact of other fractional operators like Caputo–Fabrizio fractional derivatives and comparisons with the ABC operator will be considered on the same model or other relevant models with optimal control.

Data availability statement. All data generated or analysed during this study are included in this published article.

Competing interests. The authors declare that there is no conflict of interest.

References

[1] Abdeljawad, T. & Baleanu, D. (2017), Integration by parts and its applications of a new nonlocal fractional derivative with Mittag-Leffler nonsingular kernel. *J. Nonlinear. Sci. Appl.* **10**(03), 1098–1107. arXiv preprint arXiv: 1607.00262.

[2] Abraha, T., Basir, F. Al, Obsu, L. L. & Torres, D. F. (2021) Pest control using farming awareness: Impact of time delays and optimal use of biopesticides. *Chaos Solitons Fract.* **146**, 110869.

[3] Alemu, K., Adugna, G., Lemessa, F. & Muleta, D. (2016) Current status of coffee berry disease (Colletotrichum kahawae Waller & Bridge) in Ethiopia. *Arch. Phytopathol. Plant Prot.* **49**(17-18), 421–433.

[4] Atangana, A. (2018) Blind in a commutative world: simple illustrations with functions and chaotic attractors. *Chaos Soliton. Fract.* **114**, 347–363.

[5] Atangana, A. & Araz, S.İ. (2020). Retracted: New numerical method for ordinary differential equations: Newton polynomial.

[6] Atangana, A. & Araz, S.İ. (2022) Step forward in epidemiological modeling: introducing the rate indicator function to capture waves. *Results Phys.* **38**, 105638.

[7] Atangana, A. & Baleanu, D. (2016) New fractional derivatives with nonlocal and non-singular kernel: theory and application to heat transfer model. *Therm. Sci.* **20**(2), 763–769. arXiv preprint arXiv: 1602.03408.

[8] Balatif, O., Boujallal, L., Labzai, A. & Rachik, M. (2020) Stability analysis of a fractional-order model for abstinence behavior of registration on the electoral lists. *Int. J. Differ. Equ.* **2020**, 1–8.

[9] Batista, D., Silva, D. N., Vieira, A., (2051) Legitimacy and implications of reducing Colletotrichum kahawae to subspecies in plant pathology. *Front. Plant Sci.* **7**(2017), 2051.

[10] Bonyah, E., Atangana, A. & Chand, M. (2019) Analysis of 3D IS-LM macroeconomic system model within the scope of fractional calculus. *Chaos Soliton. Fract. X* **2**, 100007.

[11] Bonyah, E., Gomez-Aguilar, J. & Adu, A. (2018) Stability analysis and optimal control of a fractional human African trypanosomiasis model. *Chaos Soliton. Fract.* **117**, 150–160.

[12] Bushnaq, S., Shah, K. & Alrabaiah, H. (2020) On modeling of coronavirus-19 disease under Mittag-Leffler power law. *Adv. Differ. Equ.* **1**, 487.

[13] Caputo, M. & Fabrizio, M. (2015) A new definition of fractional derivative without singular kernel. *Prog. Fract. Differ. Appl.* **1**(2), 73–85.

[14] Chen, Q., Mei, X., He, J., et al. (2024) Modeling and compensation of small-sample thermal error in precision machine tool spindles using spatial–temporal feature interaction fusion network. *Adv. Eng. Inform.* **62**, 102741.

[15] Cunniffe, N. J. & Gilligan, C. A. (2010) Invasion, persistence and control in epidemic models for plant pathogens: the effect of host demography. *J. R. Soc. Interface* **7**(44), 439–451.

[16] Deressa, C. T. & Duressa, G. F. (2021) Analysis of Atangana–Baleanu fractional-order SEAIR epidemic model with optimal control. *Adv. Differ. Equ.* **2021**(1), 1–25.

[17] Diethelm, K. (2010). *The Analysis of Fractional Differential Equations: An Application-Oriented Exposition Using Differential Operators of Caputo Type*, Springer, Berlin, Vol. **2004**.

[18] Diethelm, K. (2016) Monotonicity of functions and sign changes of their Caputo derivatives. *Fract. Calc. Appl. Anal.* **19**(2), 561–566.

[19] Fotsa, D., Houpa, E., Bekolle, D., Thron, C. & Ndoumbe, M. (2014) Mathematical modelling and optimal control of anthracnose. *BIOMATH* **3**(1), 1–12. arXiv preprint arXiv: 1307.1754.

[20] Fotso, Y. F., Touzeau, S., Tsanou, B., Grognard, F. & Bowong, S. (2022) Mathematical modelling of a pest in an age-structured crop model: The coffee berry borer case. *Appl. Math. Model.* **110**, 193–206.

[21] Fotso Fotso, Y., Touzeau, S., Tsanou, B., Bowong, S. & Grognard, F. (2021) Modelling and optimal strategy to control coffee berry borer. *Math. Method. App.l Sci.* **44**(18), 14569–14592.

[22] Gaitán, A. L., Cristancho, M. A., Caicedo, B. L. C., Rivillas, C. A. & Gómez, G. C. (2015). *Compendium of Coffee Diseases and Pests*, APS Press, The American Phytopathological Society.

[23] Garedew, W., Lemessa, F. & Pinard, F. (2017) Assessment of berry drop due to coffee berry disease and non-cbd factors in Arabica coffee under farmers fields of southwestern Ethiopia. *Crop Prot.* **98**, 276–282.

[24] Girma, A. & Chala, J. (2008). Resistance levels of arabica coffee cultivars to coffee berry disease, coffee wilt and leaf rust diseases in Ethiopia. In: Proceedings of the 12th Conference of the Crop Science Society of Ethiopia (CSSE), Ethiopian Institute of Agricultural Research, pp.92–103.

[25] Gong, H., Sardans, J., Huang, H., Yan, Z., Wang, Z. & Peñuelas, J. Global patterns and controlling factors of tree bark c: N: P stoichiometry in forest ecosystems consistent with biogeochemical niche hypothesis. *New Phytol.*

[26] GRIFFITHS, E., Gibbs, J. & Waller, J. (1971) Control of coffee berry disease. *Ann. Appl. Biol.* **67**(1), 45–74.

[27] Jan, R., Khan, M. A., Kumam, P. & Thounthong, P. (2019) Modeling the transmission of dengue infection through fractional derivatives. *Chaos Soliton. Fract.* **127**, 189–216.

[28] Jiang, H., Li, S. M. & Wang, W. G. (2024) Moderate deviations for parameter estimation in the fractional Ornstein-Uhlenbeck processes with periodic mean. *Acta Math. Sin. Engl. Ser.* **40**(5), 1308–1324.

[29] Khan, M. A. & Atangana, A. (2020) Modeling the dynamics of novel coronavirus (2019-Ncov) with fractional derivative. *Alex. Eng. J.* **59**(4), 2379–2389.

[30] Mbogne, D. J. F. & Thron, C. (2015) Optimal control of anthracnose using mixed strategies. *Math. Biosci.* **269**, 186–198.

[31] Melese, A. S., Makinde, O. D. & Obsu, L. L. (2022) Mathematical modelling and analysis of coffee berry disease dynamics on a coffee farm. *Math. Biosci. Eng.* **19**(7), 7349–7373.

[32] Mouen Bedimo, J., Bieysse, D., Nyassé, S., Notteghem, J.-L. & Cilas, C. (2010) Role of rainfall in the development of coffee berry disease in Coffea arabica caused by Colletotrichum kahawae, in Cameroon. *Plant Pathol.* **59**(2), 324–329.

[33] Nyaberi, H., Mutuku, W., Malonza, D., Gachigua, G., et al. (2023) A mathematical model of the dynamics of coffee berry disease. *J. Appl. Math.* **2023**, 1–10.

[34] Odibat, Z. M. & Shawagfeh, N. T. (2007) Generalized Taylor's formula. *Appl. Math. Comput.* **186**(1), 286–293.

[35] Okyere, S., Prah, J. A. & Fokuo, M. O. A model of COVID-19 with underlying health condition using fraction order derivative, arXiv preprint arXiv: 2201.11659.

[36] Paul, S., Mahata, A., Karak, M., Mukherjee, S., Biswas, S. & Roy, B. (2024) Dynamical behavior of fractal-fractional order monkeypox virus model. *Franklin Open* **7**, 100103.

[37] Paul, S., Mahata, A., Mukherjee, S., et al. (2024) Study of fractional order sir model with MH type treatment rate and its stability analysis. *Bulletin Biomath.* **2**(1), 85–113.

[38] Paul, S., Mahata, A., Mukherjee, S., Mahato, S. K., Salimi, M. & Roy, B. (2023). Study of Fuzzy Fractional Caputo Order Approach to Diabetes Model, In: *Fuzzy Optimization, Decision-Making and Operations Research*, Theory and Applications, Springer, pp. 423–434.

[39] Paul, S., Mahata, A., Mukherjee, S., Mali, P. C. & Roy, B. (2023) Fractional order SEIQRD epidemic model of Covid-19: A case study of Italy. *PLoS One* **18**(3), e0278880.

[40] Shi, X., Ishtiaq, U., Din, M. & Akram, M. (2024) Fractals of interpolative Kannan mappings. *Fractal Fract.* **8**(8), 493.

[41] Silva, M., Nicole, M., Rijo, L., Geiger, J. & Rodrigues, C. jr. (1999) Cytochemical aspects of the plant–rust fungus interface during the compatible interaction Coffea arabica (cv. caturra)–Hemileia vastatrix (race iii). *Int. J. Plant Sci.* **160**(1), 79–91.

[42] Singh, H. (2020) Analysis for fractional dynamics of Ebola virus model. *Chaos Soliton. Fract.* **138**, 109992.

[43] Singh, H. (2021) Analysis of drug treatment of the fractional HIV infection model of CD4+ T-cells. *Chaos Soliton. Fract.* **146**, 110868.

[44] Singh, H., Srivastava, H., Hammouch, Z. & Nisar, K. S. (2021). Numerical simulation and stability analysis for the fractional-order dynamics of Covid-19. *Results phys.* **20**, 103722.

[45] Sujaritpong, O., Yoo-Kong, S. & Bhadola, P. (2021). Analysis and dynamics of the international coffee trade network, In: *Journal of Physics: Conference Series*, Vol. **1719**, IOP Publishing, pp. 012106.

[46] Sweilam, N., Al-Mekhlafi, S. & Baleanu, D. (2019) Optimal control for a fractional tuberculosis infection model including the impact of diabetes and resistant strains. *J. Adv. Res.* **17**, 125–137.

[47] Teklu, S. W. (2023) Analysis of fractional order model on higher institution students' anxiety towards mathematics with optimal control theory. *Sci. Rep.* **13**(1), 6867.

[48] Tilahun, G. T., Wolle, G. A. & Tofik, M. (2021) Eco-epidemiological model and analysis of potato leaf roll virus using fractional differential equation. *Arab J. Basic Appl. Sci.* **28**(1), 41–50.

[49] Toufik, M. & Atangana, A. (2017) New numerical approximation of fractional derivative with non-local and non-singular kernel: Application to chaotic models. *Eur. Phys. J. Plus* **132**(10), 1–16.

[50] Van den Driessche, P. & Watmough, J. (2002) Reproduction numbers and sub-threshold endemic equilibria for compartmental models of disease transmission. *Math. Biosci.* **180**(1-2), 29–48.

[51] Vieira, A., Silva, D. N., Várzea, V., Paulo, O. S. & Batista, D. (2018) Novel insights on colonization routes and evolutionary potential of Colletotrichum kahawae, a severe pathogen of Coffea arabica. *Mol. Plant Pathol.* **19**(11), 2488–2501.

[52] Wang, Q., Xiang, X. & Chen, B. (2024) Food protein based nanotechnology: From delivery to sensing systems. *Curr. Opin. Food Sci.* **56**, 101134.